

# Modeling of Transport Phenomena during Hydrogen Uptake in an Alanate Storage System Equipped With Metallic Honeycomb Heat Exchanger

Maha Bhouri<sup>\*1</sup>, Jacques Goyette<sup>1</sup>, Bruce J. Hardy<sup>2</sup> and Donald L. Anton<sup>2</sup>

<sup>1</sup>Hydrogen Research Institute, UQTR, Trois-Rivières, Québec, Canada, <sup>2</sup>Savannah River National Laboratory, South Carolina, United States.

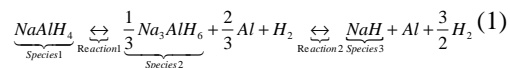
\*Corresponding author: 3351, boul. des Forges, C.P. 500, Trois-Rivières (QC), Canada G9A 5H7, maha.bhouri@uqtr.ca

**Abstract:** In this paper, we study the use of a metallic honeycomb structure is used as a heat exchanger to improve the hydrogen refueling time for an alanate storage system. Using COMSOL software, the heat exchanger structure and the hydride bed are modeled as a two separate media and the governing equations describing the physics phenomena occurring during the loading process, are solved. The simulation results showed that connecting the metallic structure to an external cooling source yields a better heat management and, therefore, refueling time. However, the hydrogen loading rate is still lower than one predicted by the kinetics model. An efficient use of the storage media can however be obtained by increasing the thermal conductivity of the hydride.

**Keywords:** Hydrogen storage, alanate hydride, modeling, metallic honeycomb structure, heat and mass transfer.

## 1. Introduction

Solid hydrogen storage systems are considered as a promising solution to facilitate safe deployment of hydrogen commercial technology. Among materials offering the ability of absorbing hydrogen in a reversible process, the Ti-doped sodium hydride is a good candidate with a theoretical hydrogen capacity of 5.5 wt% [1, 2]. Considering the charge process, the total reaction is exothermic and consists of absorbing hydrogen through a series of formation reactions



Due to the poor thermal conductivity of this material [3] and the heat generated by chemical reactions, the heat management is a key element for an effective use of such a storage system. The storage media must be maintained under

temperature and pressure conditions favorable to the absorption kinetics if one wishes to achieve a fast charging rate.

The optimization of heat transfer in solid storage media has been extensively studied in the literature for different types of heat exchangers such as aluminum foam [4], fins [5, 6], cooling tubes [5, 7-11] or by combining the effects of different cited solutions [12-20]. The majority of these numerical studies have been done on the AB<sub>5</sub> metal hydrides and the proposed configurations are especially developed with the flexibility of the numerical tool to model more complex geometries. However, for any storage media, it is sufficient to know its kinetics to optimize the corresponding hydrogen charging rate for the selected geometric configuration.

The aim of this paper is to study the heat transfer in alanate storage system equipped with a metallic honeycomb structure as heat exchanger. This structure is mainly used for applications such as structural load support, thermal management, impact energy absorption and sound absorption [22, 23]. In our case, it is used to enhance heat transfer inside the storage bed. The charging rates for storage system are compared for two cases, with and without external cooling. Moreover, the best value of the thermal conductivity resulting in the optimised charging rate is determined.

## 2. Numerical Model

### 2.1. Use of COMSOL Multiphysics

The storage system is filled with TiCl<sub>3</sub> catalyzed sodium alanate, NaAlH<sub>4</sub> and equipped with an aluminum hexagonal structure characterized by an hexagonal cell length  $l$  of 25.4mm and an hexagonal cell thickness  $t$  of 1mm. The hydride powder packs each hexagon. The heat exchanger structure and the hydride bed are modeled as a two separate media. Using the

symmetry properties, the studied domain is reduced to the 1/12 of the storage system section as illustrated in Fig.1. When the external cooling is considered, the hexagonal structure is supposed to be connected to an aluminum layer of 1mm of thickness covering the external wall of the storage system and that is maintained at a constant temperature.

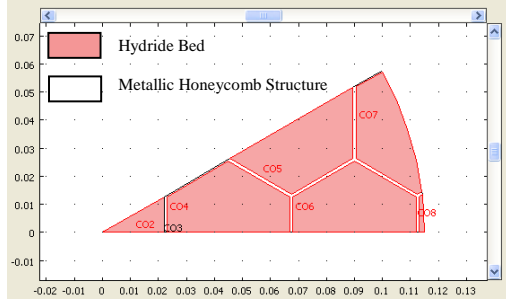


Figure.1. Section of the storage system equipped with the hexagonal structure geometry used in modeling.

## 2.2. Governing Equations

The mathematical model describing the physical phenomena occurring in the storage media is developed based on these assumptions:

- a) The hydrogen flows axially in the metal hydride.
- b) Hydrogen is assumed as in ideal gas as the pressure within the bed is moderate.
- c) The media bed does not expand or contract.
- d) The thermal properties of the bed do not change with the amount of hydrogen loading.
- e) The thermo-physical proprieties are independent of bed temperature and concentration.
- f) The characteristics of the bed are unaffected by the number of loading–unloading cycles.
- g) There is local thermal equilibrium between the hydride and hydrogen gas.
- h) The thermal conductivity, specific heat and viscosity of hydrogen do not vary with pressure over the operational regime of the storage system.
- i) The honeycomb metallic structure is composed of 6063 T83 aluminum.
- j) Thermal contact resistance is neglected between the bed and the honeycomb, and the honeycomb and the external metallic layer.
- k) The bed void fraction remains constant and uniform throughout.

The equation of state for the gas phase is expressed by the ideal gas relation

$$P = CRT \quad (1)$$

Based on this equation, the dimensionless concentration of hydrogen  $C_{nd}$  is obtained

$$C_{nd} = \frac{PT_{ref}}{P_{ref}T} \quad (2)$$

The hydrogen mass balance is given by

$$\frac{\partial C_{nd}}{\partial t} + \nabla \cdot (C_{nd} \vec{V}) = \frac{1}{C_{ref}} \left( \frac{S_{H_2}}{\varepsilon} \right) \quad (3)$$

where  $S_{H_2}$  is the source rate for hydrogen

$$S_{H_2} = \frac{1}{2} \frac{dC_3}{dt} - \frac{dC_1}{dt} \quad (4)$$

The hydrogen velocity is obtained from the Blake-Kozeny equation

$$\vec{V} = \frac{D_p^2}{150\mu} \left( \frac{\varepsilon}{1-\varepsilon} \right)^2 \nabla P \quad (5)$$

$C_1$  and  $C_3$  are respectively the concentrations of  $\text{NaAlH}_4$  and  $\text{NaH}$ . Their temporal variation is obtained from the kinetics model developed by UTRC<sup>TM</sup> [21]. Note that the kinetics model is not presented in this paper for brevity.

The energy equations in the metallic honeycomb structure and the storage media can be expressed as

$$\rho_{metal} C_{p\ metal} \frac{\partial T_{metal}}{\partial t} + \nabla \cdot (-k_{metal} \nabla T_{metal}) = 0 \quad (6)$$

$$\begin{aligned} & \rho_{bed} C_{p\ bed} \frac{\partial T_{nd}}{\partial t} + \nabla \cdot (-k_{bed} \nabla T_{nd}) = \\ & -\varepsilon \rho_{H_2} C_{p\ H_2} \left( \frac{\partial T_{nd}}{\partial t} + \vec{V} \cdot \nabla T_{nd} \right) \\ & + \frac{1}{T_{ref}} \left( \frac{\partial P}{\partial t} + \varepsilon \vec{V} \cdot \nabla P \right) + \frac{1}{T_{ref}} S_T \end{aligned} \quad (7)$$

where  $S_T$  is the reaction enthalpy term:

$$S_T = \frac{dC_1}{dt} \Delta H_{Run1} - 0.5 \frac{dC_3}{dt} \Delta H_{Run2} \quad (8)$$

The weight fraction of stored hydrogen is given by

$$\begin{aligned} wf &= \frac{\text{Mass of } H_2 \text{ contained in metal}}{\text{Equivalent mass of } NaAlH_4} \\ &= \frac{1.5(C_1 + C_2)}{C_{eqv}} \frac{M_{H_2}}{M_{NaAlH_4}} \end{aligned} \quad (9)$$

## 2.3. Initial and boundary conditions

Initially, hydrogen, sodium hydride and metallic structure are at the same temperature.

$$T_{metal} = T_{bed} = 100 \text{ } ^\circ\text{C} \quad (10)$$

The bed is composed of pure NaH

$$C_{3,0} = 13333.33 \text{ mol/m}^3 \quad (11)$$

The bed pressure is 1 bar. Due to the flow of hydrogen, it increases exponentially with time within the first 10 s and then remains at a constant value of 50 bar.

On the surfaces of symmetry, a Neumann boundary condition is applied

$$\left( C_{nd} \vec{V} \right) \cdot \vec{n} = 0 \quad (11)$$

The continuity conditions are applied to all interfaces between honeycomb structure and hydride bed

$$\vec{n} \cdot (k_{metal} \nabla T_{metal}) = \vec{n} \cdot (k_{bed} \nabla T_{bed}) \quad (12)$$

The external wall and the surfaces of symmetry are thermally insulated

$$\vec{n} \cdot (k_{bed} \nabla T_{nd}) = 0 \quad (13)$$

When the configuration includes the metallic layer, it is assumed that the external wall is maintained at a constant temperature of 100 °C.

Based on the empirical kinetics model developed by the United Technology Research Center, UTRC<sup>TM</sup> [21], the set of equations corresponding to this model are defined in COMSOL Multiphysics 3.5a as PDE and solved as a 0-dimension model. After that, these results will be used to compare and optimize the hydrogen charging rates obtained from the different studied configurations.

### 3. Results

As mentioned above, the storage media is TiCl<sub>3</sub> catalyzed sodium alanate, NaAlH<sub>4</sub>. The numerical results of the 0-dimension model are compared to UTRC<sup>TM</sup> experimental data and a good agreement is obtained as shown in Fig.2.

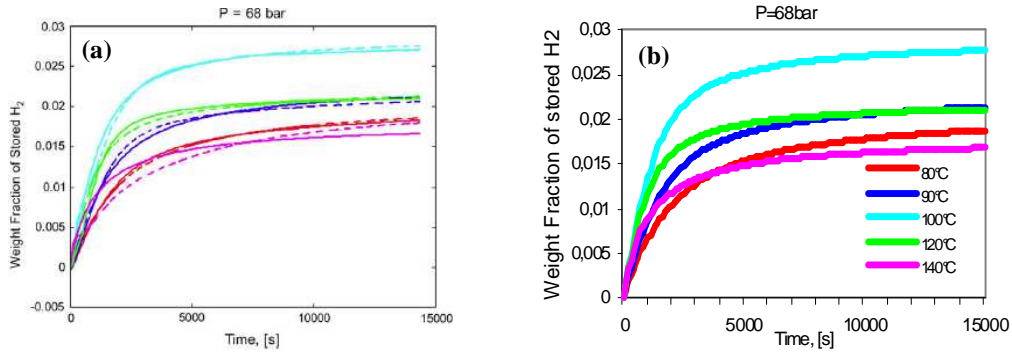


Figure.2. Comparison of the H<sub>2</sub> absorption curves (a) UTRC<sup>TM</sup> experimental data [21] and (b) obtained from the 0-dimension model, for the same pressure and range of temperature.

Figs. 3.(a), (b), (c) show the distributions of the hydride temperature and the concentrations of formed species at selected times 40 s, 120 s and 720s. Due to the exothermic reactions, temperature increases throughout the hydride bed as illustrated in Fig.3.(a). It reaches its maximum at the center of each hexagon, while the outer part is colder due to the contact with the metal structure. Indeed, this structure acts as a sink for absorbing the reaction heat. Thus, during 120 s, a temperature difference of 13 °C between the temperature of hexagonal structure and the metal hydride is noted. After 720 s, this difference is reduced to 2.5 °C although the temperature reaches 221°C.

The evolution of the hexa- and tetra-hydrides are shown in Fig.3.(b), (c)). The formation of these species is the slowest in the middle of each

hexagon where the reaction speed is reduced by the increase of the hydride bed temperature. From Fig.3.(b), it is seen that the Na<sub>3</sub>AlH<sub>6</sub> concentration increases over time, particularly in areas in contact with metal walls. The NaAlH<sub>4</sub> concentration follows the same behavior, however, at t=720 s, there is a decrease of this concentration relative to prior time (Fig.3.(c)). This suggests that reaction 2 is reversed due to the drastic increase of the hydride bed temperature.

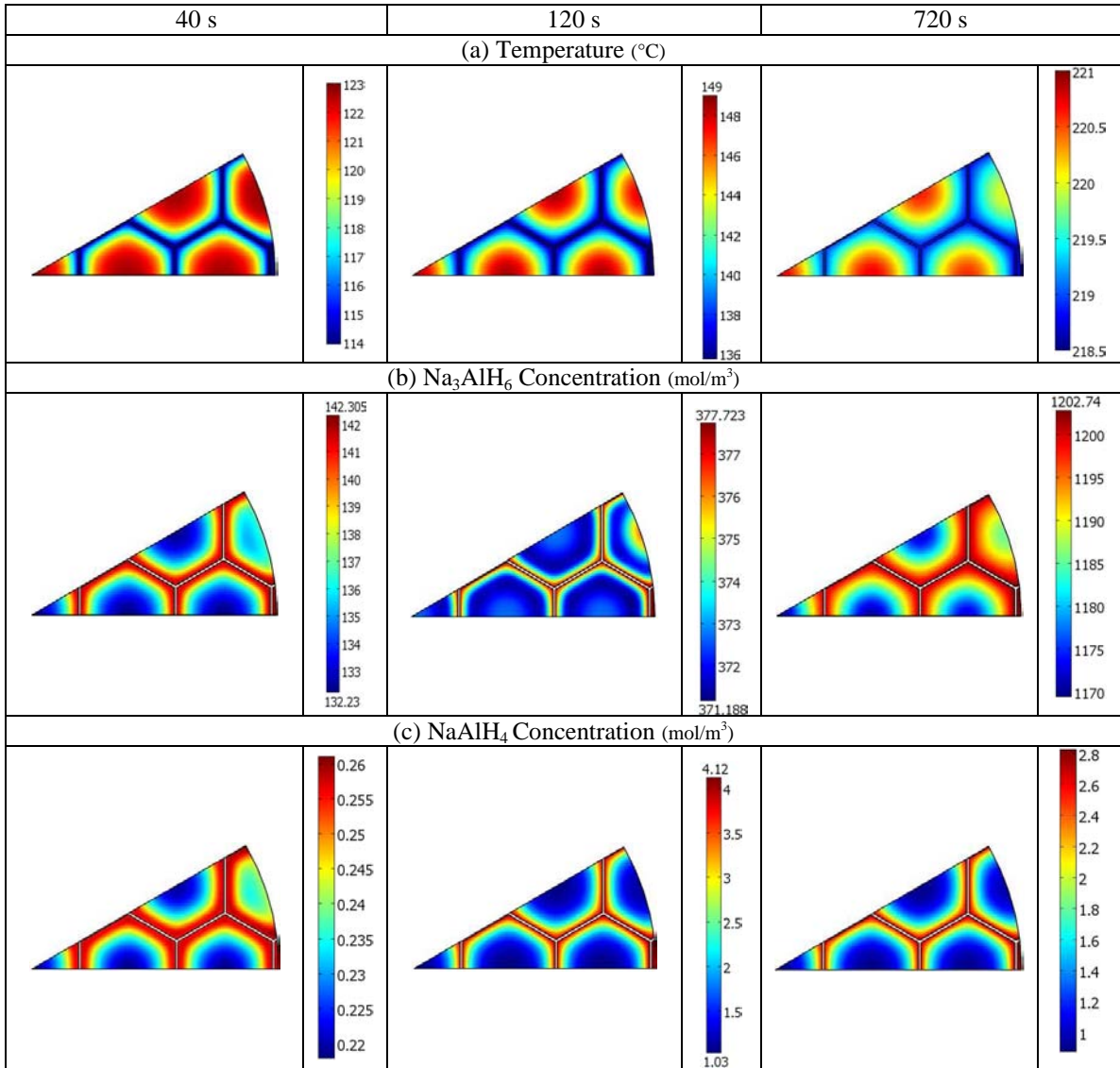


Figure.3. Evolution of the temperature and species concentrations at selected times, case without external cooling.

The metallic honeycomb structure can also act as a bridge to dissipate the heat if it is connected to an external cooling source. In this case, the outer wall of the tank is assumed to be covered with a thin layer of aluminum maintained at 100 °C and in

close contact with the honeycomb structure. The distribution of the hydride bed temperature and the species concentration at 720 s are illustrated in Fig.4.

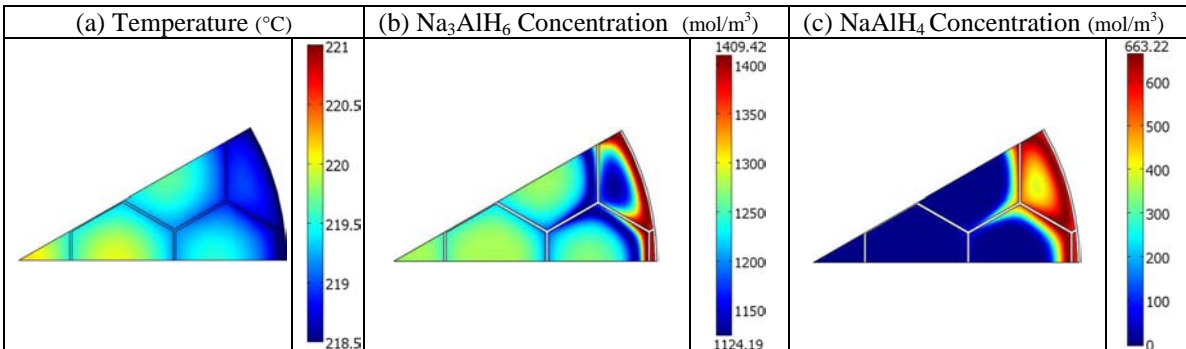


Figure.4. Evolution of the temperature and species concentrations at 720 s, case with external cooling.

In the presence of the external cooling source, the maximum temperature does not exceed 181 °C, a decrease of 40 °C compared to the basic case. The concentrations  $\text{Na}_3\text{AlH}_6$  and  $\text{NaAlH}_4$  reach a maximum of  $1409 \text{ mol/m}^3$  and  $663 \text{ mol/m}^3$  in the outer region of the tank. However, their distribution is not uniform throughout the hydride bed. This is most notable for the tetrahydride. Indeed, this species is formed at the periphery while, at the same time, it is decomposed within the hydride bed.

To better understand the physical phenomena occurring in the hydride bed, the averaged profiles of temperature and pressure equilibrium in the hydride bed are presented in Figures 5 and 6.

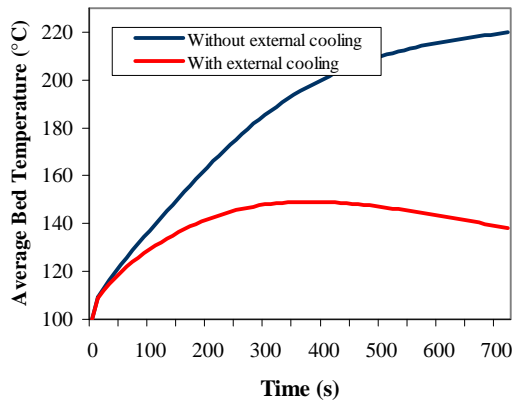


Figure.5. Time evolution of average bed temperature, cases without and with external cooling.

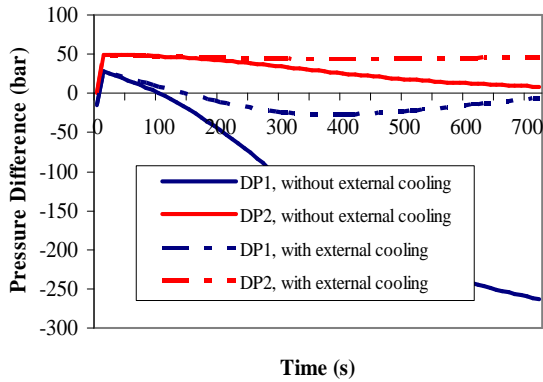


Figure.6. Time evolution of the difference between the average hydrogen bed pressure and hydrogen equilibrium pressures, cases without and with external cooling.

From Fig.5, a large gap between the average temperatures corresponding to the cases without and with external cooling is observed. In the absence of any cooling source, the average temperature follows an increasing trend during 720 s. With an external cooling, the average temperature reaches a maximum of 149 °C at 410 s. Thereafter; it decreases to move towards the coolant temperature.

The variation of the bed temperature can influence the charging process. The absorption of hydrogen takes place if the pressure of hydrogen in the hydride bed is larger than the equilibrium pressures of reactions 1 and 2. Otherwise, the reactions can be excessively slow or even reverse. The equilibrium pressures are given by the vant'Hoff equation:

$$P_{eq1}(T) = 10^5 \exp\left[\frac{\Delta H_1}{RT} - \frac{\Delta S_1}{R}\right] \quad (14)$$

$$P_{eq2}(T) = 10^5 \exp\left[\frac{\Delta H_2}{RT} - \frac{\Delta S_2}{R}\right]$$

Fig.6 shows the differences between the pressure in the bed and the equilibrium pressures. For the base case, the absorption of hydrogen is due essentially to the formation of  $\text{Na}_3\text{AlH}_6$ . After 720 s, the difference DP2 becomes very small indicating that the kinetics of reaction 1 is very slow. Concerning the formation of the  $\text{NaAlH}_4$ , the difference DP1 is positive only for the first 100 s. After this, the equilibrium pressure  $P_1$  exceeds that of the hydride bed and the formed tetrahydride decomposes, which is consistent with the concentration profile of  $\text{NaAlH}_4$  already presented in Fig.3.(c).

In the case with external cooling, the difference between the bed pressure and the equilibrium pressure, DP2 is almost constant throughout the simulation time and the kinetics of the  $\text{Na}_3\text{AlH}_6$  formation is not slowed down. However, for the formation of the  $\text{NaAlH}_4$ , there is always a reversal of this reaction even though the gap DP1 is reduced compared to the case without external cooling.

The bed weight fractions of the two cases are plotted and compared to one obtained from the 0-Kinetics model as illustrated in Fig.7.

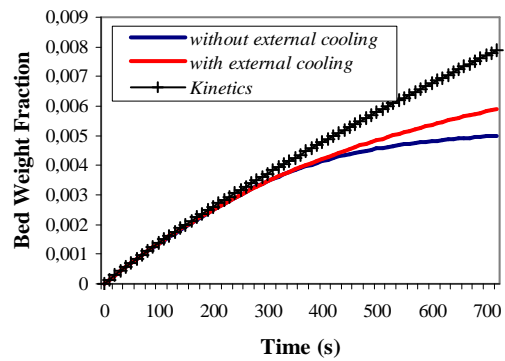


Figure.7. Comparison of the bed weight fraction of stored hydrogen for cases without and with external cooling.

During the first 410 s, the two curves are indistinguishable. From that moment on, the gap between the curves of the bed weight fraction becomes significant. This is the moment when the average temperature of the hydride bed starts to decrease, in the case of external cooling (Fig.5).

This represents an increase of 18% of storage capacity but remains lower than that obtained by the kinetic model.

An efficient use of the storage system can be obtained by increasing the thermal conductivity of the hydride. A comparison between the different bed weight fraction are presented in Fig.8 where the thermal conductivity is varied from 0.325 W/(m.K) to 10.4 W/(m.K).

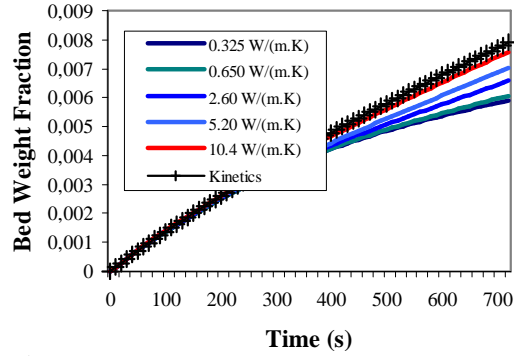


Figure 8. Comparison of the bed weight fraction of stored hydrogen for different bed thermal conductivity, cases with external cooling.

When the thermal conductivity is increased to 10.4 W/(m.K), the heat is conducted efficiently from the powder to the honeycomb structure connected to the external wall maintained at  $T_{wall} = 100\text{ }^{\circ}\text{C}$ . In this case, the charging rate is similar to one obtained from the kinetics model.

#### 4. Conclusion

In this paper, heat transfer in an alanate storage system equipped with a metallic honeycomb structure has been modeled. Simulation results shows that the metallic structure acts as a heat sink during the first instant of the reaction, after that, it becomes in thermal equilibrium with the hydride bed. It is necessary to connect this structure to an external cooling source to enhance its efficiency. In this case, an improvement of 18% in the charging rate can be obtained. For the same configuration, an effective use of the storage system can be obtained if the thermal conductivity is increased to 10.4 W/(m.K). Future studies will be focused on a parametric analysis to evaluate the influence of other parameters, such as cell length, cell thickness of the metallic structure and the possibility to manage the released heat by equipping the storage system with an internal cooling source.

#### 5. Acknowledgement

M.B. would like to thank the Canadian International Development Agency for a graduate student fellowship. This work was funded in part by the NSERC Hydrogen Canada (H<sub>2</sub>CAN) Strategic

Research Network and by Natural Resources Canada.

B.J.H. and D.L.A. wish to acknowledge the support and funding of the United States Department of Energy through the Hydrogen Storage Engineering Center of Excellence.

#### 6. Nomenclature

$C$	concentration of H <sub>2</sub> in the bed void space, mol H <sub>2</sub> /m <sup>3</sup>
$C_{eq}$	equivalent concentration of NaAlH <sub>4</sub> [mol/m <sup>3</sup> ] based on the initial concentrations of all metal species
$C_{nd}$	the non-dimensionalized concentration of H <sub>2</sub> = $C / C_{ref}$
$C_{p\text{H}_2}$	specific heat of H <sub>2</sub> , J/(kg K)
$C_{p\text{metal}}$	specific heat of the metal, J/(kg K)
$C_1$	bulk concentration of NaAlH <sub>4</sub> , mol/m <sup>3</sup>
$C_2$	bulk concentration of Na <sub>3</sub> AlH <sub>6</sub> , mol/m <sup>3</sup>
$C_3$	bulk concentration of NaH, mol/m <sup>3</sup>
$D_p$	mean diameter of particles in bed, m
$k_{bed}$	bed thermal conductivity, W/(m K)
$k_{metal}$	thermal conductivity of the metal, W/(m K)
$\vec{n}$	outward normal to surface
$P$	pressure, Pa
$P_{nd}$	$P / P_{ref}$ = non-dimensional pressure
$P_{eq1}(T)$	H <sub>2</sub> pressures in equilibrium at temperature, $T$ , with the NaAlH <sub>4</sub> , Pa
$P_{eq2}(T)$	H <sub>2</sub> pressures in equilibrium at temperature, $T$ , with the Na <sub>3</sub> AlH <sub>6</sub> , Pa
$P_{ref}$	reference pressure, Pa
$R$	gas constant = 8.314 J/(mol K)
$S_{T_{nd}}$	Enthalpy change due to chemical reactions, W/m <sup>3</sup>
$t$	time, s
$T$	temperature, K
$T_{nd}$	$T / T_{ref}$ = non-dimensional temperature
$T_{ref}$	reference temperature, K
$T_{wall}$	tube wall temperature, K
$\vec{V}$	mean interstitial H <sub>2</sub> velocity, m/s
Greek	
$\Delta H_i$	enthalpy of reaction on a molar basis of species $i$ , J/(mol of $i$ )
$\Delta H_{Rxn1}$	heat of reaction per mol of H <sub>2</sub> consumed going to left for reaction 1
$\Delta H_{Rxn2}$	heat of reaction per mole of H <sub>2</sub> consumed going to left for reaction 2
$\epsilon$	void fraction (porosity) of particle bed
$\mu$	viscosity of H <sub>2</sub> , Pa s

$\rho$	mass density, kg/m <sup>3</sup>
$\rho_{bed}$	bulk mass density of bed; kg/m <sup>3</sup> = $(1 - \epsilon)\rho_{bed-particulate}$ = mass of solid/total volume
$\rho_{bed-particulate}$	particle mass density of bed, kg/m <sup>3</sup> = mass of solid/volume of solid
$\rho_{bed} C_{p\ bed}$	$\rho_{Solid\ Reactants} C_{p\ Solid\ Reactants} + \rho_{Solid\ Products} C_{p\ Solid}$
$\rho_{H_2}$	hydrogen density, kg/m <sup>3</sup>
$\rho_{metal}$	density of the metal, kg/m <sup>3</sup>

Symbol and operators

$\nabla$  gradient, 1/m.

## 7. References

1. Borislav Bogdanovic, M.S., Ti-doped alkali metal aluminium hydrides as potential novel reversible hydrogen storage materials. *Journal of Alloys and Compounds*, 1997 253-254: p. 1-9.
2. Borislav Bogdanovic, R.A.B., Ankica Marjanovic, Manfred Schwickardi, Joachim Tölle, Metal-doped sodium aluminium hydrides as potential new hydrogen storage materials. *Journal of Alloys and Compounds*, 2000. 302(1-2): p. 36-58.
3. D.E. Dedrick, M.P.K., B.C. Replogle, K.J. Gross, Thermal properties characterization of sodium alanates. *Journal of Alloys and Compounds*, Volume , Issues , 8 March , Pages 2005. 389(1-2): p. 299-305.
4. F. Laurencelle, J.G., Simulation of heat transfer in a metal hydride reactor with aluminium foam. *International Journal of Hydrogen Energy*, 2007. 32: p. 2957 - 2964.
5. Brendan D. MacDonald, A.M.R., A thermally coupled metal hydride hydrogen storage and fuel cell system. *Journal of Power Sources*, 2006. 161: p. 346-355.
6. Kaplan, Y., Effect of design parameters on enhancement of hydrogen charging in metal hydride reactors. *International Journal of Hydrogen Energy*, 2009. 34(5): p. 2288-2294.
7. A. Demircan, M.D., Y. Kaplan, M.D. Mat, T.N. Veziroglu, Experimental and theoretical analysis of hydrogen absorption in LaNi<sub>5</sub>-H<sub>2</sub> reactors. *International Journal of Hydrogen Energy*, 2005. 30(13-14): p. 1437-1446.
8. Muhittin Bilgili, Ö.E.A., Numerical analysis of hydrogen absorption in a P/M metal bed. *Powder Technology*, 2005. 160(2): p. 141-148.
9. P. Muthukumar, U.M.a.A.D., Parametric studies on a metal hydride based hydrogen storage device, *International Journal of Hydrogen Energy*, 2007. 32(18): p. 4988-4997.
10. G. Mohan, M.P.M., S. Srinivasa Murthy, Performance simulation of metal hydride hydrogen storage device with embedded filters and heat exchanger tubes. *International Journal of Hydrogen Energy*, 2007. 32: p. 4978 - 4987.
11. A. Freni, F.C., G. Cacciola, Finite element-based simulation of a metal hydride-based hydrogen storage tank. *International Journal of Hydrogen Energy*, 2009 34(20): p. 8574-8582.
12. M. Gambini, M.M., M. Vellini, Numerical analysis and performance assessment of metal hydride-based hydrogen storage systems. *International Journal of Hydrogen Energy*, 2008. 33(21): p. 6178-6187.
13. C.A. Chung, C.-S.L., Prediction of hydrogen desorption performance of Mg<sub>2</sub>Ni hydride reactors. *International Journal of Hydrogen Energy*, 2009. 34(23): p. 9409-9423.
14. F. Askri, M.B.S., A. Jemni, S. Ben Nasrallah, Optimization of hydrogen storage in metal-hydride tanks. *International Journal of Hydrogen Energy*, 2009. 34(2): p. 897-905.
15. S. Mellouli, H.D., F. Askri, A. Jemni, S. Ben Nasrallah, Hydrogen storage in metal hydride tanks equipped with metal foam heat exchanger. *International Journal of Hydrogen Energy*, 2009 34(23): p. 9393-9401.
16. S. Mellouli, F.A., H. Dhaou, A. Jemni, S. Ben Nasrallah, Numerical study of heat exchanger effects on charge/discharge times of metal-hydrogen storage vessel. *International Journal of Hydrogen Energy*, 2009. 34(7): p. 3005-3017.
17. S. Mellouli, F.A., H. Dhaou, A. Jemni, S. Ben Nasrallah, Numerical simulation of heat and mass transfer in metal hydride hydrogen storage tanks for fuel cell vehicles. *International Journal of Hydrogen Energy*, 2010. 35(4): p. 1693-1705.
18. Timothée L. Pourpoint, V.V., Issam Mudawar, Yuan Zheng, Timothy S. Fisher, Active cooling of a metal hydride system for hydrogen storage. *International Journal of Heat and Mass Transfer*, 2010. 53(7-8): p. 1326-1332.
19. Bruce J. Hardy, D.L.A., Hierarchical methodology for modeling hydrogen storage systems. Part II: Detailed models. *International Journal of Hydrogen Energy*, 2009. 34(7): p. 2992-3004.
20. Ch. Veerajug, M.R.G., Heat and mass transfer studies on plate fin-and-elliptical tube type metal hydride reactors. *Applied Thermal Engineering*, 2010. 30(6-7): p. 673-682.
21. Bruce J. Hardy, D.L.A., Hierarchical methodology for modeling hydrogen storage systems. Part I: Scoping models. *International Journal of Hydrogen Energy*, 2009. 34(5): p. 2269-2277.
22. T. Wen, J.T., T.J. Lu, D.T. Queheillalt, H.N.G. Wadley, Forced convection in metallic honeycomb structures. *International Journal of Heat and Mass Transfer*, 2006. 49(19-20): p. 3313-3324.
23. Shutian Liu, Y.Z., Peng Liu, New analytical model for heat transfer efficiency of metallic honeycomb structures. *International Journal of Heat and Mass Transfer*, 2008. 51(25-26): p. 6254-6258.